Molecular Neurobiology (2019) 56:2234–2243
https://doi.org/10.1007/s12035-018-1224-4

Chemotherapy-Induced Cognitive Impairment Is Associated with Cytokine Dysregulation and Disruptions in Neuroplasticity

Dong-Dong Shi[1] · Yu-Hua Huang[2] · Cora Sau Wan Lai[2] · Celia M. Dong[3] · Leon C. Ho[3] · Ed X. Wu[3] · Qi Li[4] · Xiao-Min Wang[5] · Sookja Kim Chung[2] · Pak Chung Sham[6] · Zhang-Jin Zhang[1]

Received: 6 January 2018 / Accepted: 3 July 2018 / Published online: 14 July 2018

Abstract

Chemotherapy-induced cognitive impairment, often referred to as "chemobrain," is a common side effect. In this study, mice received three intraperitoneal injections of a combination of docetaxel, adriamycin, and cyclophosphamide (DAC) at 2-day intervals. A water maze test was used to examine cognitive performance, and manganese-enhanced magnetic resonance imaging (MEMRI) was used to examine hippocampal neuronal activity. The whole brain, prefrontal cortex, hippocampus, and blood samples were then collected for cytokine measurement. The DAC-treated mice displayed a significantly shorter duration spent in and fewer entries into the target quadrant of the water maze than the control mice and a pronounced decrease in MEMRI signal intensity in the hippocampal subregions. In a separate experiment using in vivo transcranial two-photon imaging, DAC markedly eliminated dendritic spines without changing the rate of spine formation, leading to a striking loss of spines in the medial prefrontal cortex. DAC treatment resulted in significant elevations in the levels of the proinflammatory cytokines interleukin 6 (IL-6) and tumor necrosis factor-α (TNF-α) and in significant decreases in the levels of the anti-inflammatory cytokines IL-4 and IL-10 in most of the sera and brain tissues examined. The IL-6 and TNF-α levels of several sera and brain tissues showed strong inverse correlations with the duration and number of entries in the target quadrant of the water maze and with the hippocampal MEMRI signal intensity, but also showed striking positive correlations with spine elimination and loss. These results indicate that chemobrain is associated with cytokine dysregulation and disrupted neuroplasticity of the brain.

Keywords Chemotherapy · Cognitive impairment · Cytokines · Neuroplasticity · Manganese-enhanced magnetic resonance imaging (MEMRI) · In vivo transcranial two-photon imaging

Introduction

Chemotherapy-induced cognitive impairment, often referred to as "chemobrain," is a potential common side effect that manifests clinically as difficulty in learning, memory, attention, processing speed, concentration, and executive function [1, 2]. Estimates indicate that up to 75% of cancer patients have reported acute cognitive symptoms during chemotherapy

Electronic supplementary material The online version of this article (https://doi.org/10.1007/s12035-018-1224-4) contains supplementary material, which is available to authorized users.

✉ Zhang-Jin Zhang
zhangzj@hku.hk

[1] School of Chinese Medicine, LKS Faculty of Medicine, The University of Hong Kong, 10 Sassoon Road, Pokfulam, Hong Kong, China

[2] School of Biomedical Sciences, State Key Laboratory of Pharmaceutical Biotechnology, LKS Faculty of Medicine, The University of Hong Kong, Hong Kong, China

[3] Laboratory of Biomedical Imaging and Signal Processing, Department of Electrical and Electronic Engineering, The University of Hong Kong, Hong Kong, China

[4] Department of Psychiatry, State Key Laboratory of Cognitive and Brain Sciences, HKU-SIRI, The University of Hong Kong, Hong Kong, China

[5] Department of Anesthesiology, LKS Faculty of Medicine, The University of Hong Kong, Hong Kong, China

[6] Department of Psychiatry, State Key Laboratory of Cognitive and Brain Sciences, Genome Research Centre, The University of Hong Kong, Hong Kong, SAR, China

[1, 2]. Due to the recent tremendous improvement in survival rate and the feasibility of follow-up, cognitive deficits have been found to be particularly evident in breast cancer patients compared to those with other cancers [3]. Numerous previous studies have examined the effects of single and different combinations of chemotherapies on cognitive function of animals, and consistently demonstrated the performance impairment in hippocampus-related learning and memory tasks following treatment [4–7]. While most animal studies focused on cell-biological and metabolic effects of cytostatic treatment with common cancer chemotherapeutics and did not target a specific cancer condition [4–7], one recent study has revealed that both chemotherapy and tumor itself could contribute to cognitive impairment in a transgenic mouse model of breast cancer [8]. The present study was then designed to further develop an animal model that could specifically mimic acute cognitive impairment with a commonly used chemotherapeutic regimen for the treatment of breast cancer.

Cytokine dysregulation is thought to play an important role in the pathogenesis of chemobrain [9]. Chemotherapy can induce an immune reaction that subsequently causes highly elevated levels of various cytokines via a positive feedback loop between cytokines and white blood cells [10]. Small quantities of chemotherapeutic drugs can cross the blood-brain barrier and enter the brain, resulting in overproduction of proinflammatory cytokines, such as interleukin 6 (IL-6) and tumor necrosis factor-α (TNF-α), and suppression of anti-inflammatory cytokines, such as IL-4 and IL-10. Proinflammatory cytokines elicited by chemotherapy of peripheral normal and tumor tissues also can cross the blood-brain barrier, damage neuronal cells in the brain, and disrupt the blood-brain barrier integrity and transport mechanisms, further leading to the overflow of chemotherapeutic drugs into the brain [9]. Proinflammatory cytokines have considerable toxic effects on neuronal cells, particularly those in the hippocampus and the prefrontal cortex associated with cognitive functions, as they are more susceptible to neurotoxin insults [9]. Several clinical studies have revealed that higher blood concentration of IL-6 was associated with poorer cognitive performance, but the elevated level of IL-4 was protective against chemobrain in breast cancer patients [11, 12]. TNF-α was also associated with self-reported memory complaints in breast cancer survivors [13]. One study has exhibited better cognitive performance in IL-6 deficient mice than wild-type genotype mice, confirming the detrimental effects of IL-6 [14]. Numerous neuroimaging studies have shown brain microstructural abnormalities and neural correlates of cognitive impairments in patients who had developed chemobrain and in animal models [15, 16]. These studies have led to the hypothesis that chemotherapy-induced cytokine dysregulation and disrupted neuroplasticity in related brain regions may lead to the development of chemobrain.

To test this hypothesis, a mouse model of chemobrain was established by repeated administration of a combination of docetaxel, adriamycin, and cyclophosphamide (DAC), a commonly used chemotherapeutic regimen for breast cancer [17]. Cognitive performance was tested in a water maze, and brain neuronal activity and dendritic spine plasticity were examined with manganese-enhanced magnetic resonance imaging (MEMRI) and in vivo transcranial two-photon microscopy, respectively. Blood and brain levels of proinflammatory (IL-6 and TNF-α) and anti-inflammatory (IL-4 and IL-10) cytokines were measured. Intercorrelations among behavioral, neuroimaging, and cytokine variables were further analyzed.

Materials and Methods

Animals and Experimental Procedure

The experiment protocol was approved by the Committee on the Use of Live Animals in Teaching and Research (CULATR 3531–14 and 3267–14) of LKS Faculty of Medicine of the University of Hong Kong. For different neuroimaging purposes, female C57/BL6J and Thy1-YFP H-line transgenic mice (Charles River Laboratory, USA) between 18 and 20 g were used for MEMRI scanning and in vivo transcranial two-photon microscopy, respectively. The experimental procedure is illustrated in Fig. 1S. The mice were housed three to five per cage and maintained on a 12-h light/dark cycle at 23 °C with water and food available ad libitum. Body weight was monitored during habituation, treatment, and recovery.

Treatment

Chemotherapy began after a 7-day habituation period. DAC doses used in this study were converted from doses used in humans for the treatment of breast cancer [18]. To determine an optimal DAC dosing regimen, mice received three intraperitoneal injections of one of three DAC dosing regimens (5/5/20, 10/10/40, or 15/15/60 mg/kg) (10 mice per group) at a 2-day intervals. Control groups of the two strains of mice were injected with vehicle (0.9% saline solution). The transgenic mice and their control group were treated identically. The mice remained in their cages for a 7-day recovery period after the completion of the treatment.

Due to a high mortality rate in 15/15/60-mg/kg DAC group and based on behavioral test results, 10/10/40 mg/kg DAC was chosen as the optimal dosing regimen for further in vivo neuroimaging and cytokine measurement (see below).

Behavioral Test

Following recovery, the mice were tested in an open-field apparatus to detect the effects of handling and injection on their anxiety level and locomotor activity. Their cognitive performance was then tested in a Morris water maze. All testing

was conducted between 09:00 and 12:00, videotaped, and analyzed with video tracking software (Ethovision, Noldus, Netherlands). The order of testing was random.

Open-Field Test The open-field apparatus is a 40 × 40 × 60-cm Plexiglas arena with clear walls and a white floor with a 25 × 25-cm central zone. Testing followed in dimly light condition without the presence of experimenters. The total distance and velocity moved and the frequency of transfer between the central and surrounding zones were recorded over a 10-min test period. The apparatus was cleaned with 75% alcohol between tests.

Morris Water Maze Test Cognitive performance testing consisted of four successive training trials and a probe test conducted in a Morris water maze, a white circular tank (120 cm in diameter, 50 cm in deep) filled with recycling water at a constant temperature (22 °C ± 2 °C). Prior to the first training trial, mice were given a habituation trial with a red flagging on the platform to assess any spatial bias and their basal swim speed. Four distal landmarks with different shapes and colors were placed around the tank during training days. Using the landmarks, the mice were trained to find a hidden hyaline platform (10 cm in diameter, 24 cm in high) that was submerged 1 cm below the surface of water and situated in the same location on each training day. Each mouse underwent four successive training trials with a 15-min interval each day for 5 days. Each mouse was gently released onto the water of the desired start position in the maze facing the tank wall. The start points differed each day to encourage the development of spatial memory. Each mouse's movement trajectory in the maze was recorded with the video-tracking software. The training trial ended if the mouse reached the hidden platform and remained on there for at least 10 s or if the mouse could not find the platform within 60 s. Those who could not find the platform within the defined period were guided to the platform and allowed to remain there for 15 s. The escape latency to the platform was recorded from each training trial.

The probe test was carried out 24 h after the last training trial. The platform was removed and the mouse was placed in a novel start position to ensure its spatial preference rather than that for a specific swim pathway. The mice were allowed to swim freely for 60 s. The duration spent in the targeted quadrant in which the arena platform had been located and the frequency with which the mouse entered the targeted quadrant were recorded as variables for learning and memory ability.

In Vivo Neuroimaging

MEMRI MEMRI is a powerful neuroimaging approach to investigate in vivo brain activity, neuronal tract tracing, and enhancement of anatomic detail in rodents [19]. To evaluate the hippocampus activities of DAC-treated mice, MEMRI was performed. C57/BL6J mice who had completed the behavioral tests underwent MEMRI scanning as reported previously [20]. Food and water were available before MEMRI. Briefly, the mice were given an intraperitoneal injection of $MnCl_2$ (45 mg/kg) 4 h before MEMRI. The mice were anesthetized with isoflurane (2.5% for induction and 1.0% for maintenance) and placed on a holder in the prone position with a facemask. During MRI scan, the mice were kept warm with a warming system (Bruker BioSpin MRI GmbH). The respiratory rate was continuously monitored using MRI-compatible sensors (SA instruments) and kept within a range of 90 to 110 breaths per minute.

Scanning was conducted with a 7-T MRI scanner with maximum gradient of 360 mT/m (70/16 PharmaScan, Bruker Biosin GmbH, Germany). Standard multislice coronal images were obtained with field of view of 2.5 × 2.5 cm^2, a slice thickness of 0.5 mm, a matrix of 256 × 256, and 15 continuous slices. T_1-weighted images were acquired by a RARE sequence (TR = 1366.7 ms, TE_{eff} = 7.5 ms, RARE factor = 4, NEX = 6). The signal intensity was calculated as the ratio between the mean signal in the hippocampal subregions (dentate gyrus, *Cornu Ammonis* 1 (CA1), and *Cornu Ammonis* 1 (CA30)) and the mean signal of the adjacent corpus callosum using ImageJ software (Wayne Rasband, NIH, USA). After imaging, sera were collected via cardiac puncture, and the brains were removed for cytokine measurement (see the following).

In Vivo Transcranial Two-Photon Imaging The Thy1-YFP H-line transgenic mouse strain that expresses the yellow fluorescent protein (YFP) in the nervous system have been widely used to investigate neuronal development and regeneration [21]. In this separate experiment, the transgenic mice received the 10/10/40-mg/kg DAC regimen as described previously. Spine plasticity was examined using in vivo transcranial two-photon microscopy by longitudinally observing the formation and elimination of dendritic spines of cortical layer V pyramidal neurons in the medial prefrontal cortex [22, 23]. The procedure was described in our previous studies [24]. Briefly, each mouse was anesthetized with an intraperitoneal injection of 120 mg/kg ketamine and 18 mg/kg xylazine, and its head was attached to a head-holder to prepare a thinned-skull window using a high-speed microdrill. A round window of about 0.8 mm and a skull thickness of about 20 μm were created at the medial prefrontal cortex.

Re-imaging was conducted 3 days after the initial imaging. A 25×, NA 1.05 water-immersion objective (Olympus) and a 920-nm two-photon laser were used to acquire the images. High-magnification images were scanned in a Z-stack manner (thickness, 80 to 120 μm; layer interval, 0.75 μm). For re-imaging of the same region, the thinned regions were identified based on the map of the brain vasculature, and

microsurgical blades were used to further thin the region of interest until a clear image could be obtained. The imaging region was 216 × 216 μm, and its center was located at the frontal association cortex (+ 2.8-mm bregma, + 1.0-mm midline). The captured images of dendritic spines were analyzed using ImageJ software (Wayne Rasband, NIH, USA).

The number of eliminated and newly formed spines and filopodia were counted from nine imaged areas chosen at random. The percentages of the types of spines and filopodia were calculated. The analysts were blinded to the animal treatment. After imaging, sera and brain tissues were collected for cytokine measurement (see the following).

Cytokine Measurement

After in vivo imaging, both C57/BL6J and Thy1-YFP transgenic mice were further used for cytokine measurement. A total of 0.5 to 0.6 mL of blood was collected via cardiac puncture; serum was separated immediately and stored at − 80 °C for measurement of cytokines. The mice were then perfused to drain blood from brains, decapitated, and the whole brains were removed. The hippocampus and prefrontal cortex were dissected from half of the whole brains. For cytokine measurement, the brain tissues were prepared according to the protocol provided in the enzyme-linked immunosorbent assay (ELISA) kit (Boster, China). Briefly, approximately 10 mg of tissues was homogenized in 100 μL of 0.1 M phosphate-buffered saline (PBS) containing 1% phenylmethanesulfonyl fluoride (PMSF; Sigma-Aldrich, USA) on ice for 30 min. The homogenate was then centrifuged at 20,000*g* at 4 °C for 20 min. The supernatant was separated for ELISA analysis, and the serum and brain concentrations of the four cytokines, IL-4, Il-6, IL-10, and TNF-α, were measured using an ELISA kit (Boster, China). The absorbance of each well for cytokine reactions was measured at 450 nm. The concentrations of cytokines were calculated from standard curves constructed with the four-parameter logistic curve fitting model by plotting the mean absorbance obtained for each reference standard against each cytokine concentration.

Statistical Analysis

Two-way analysis of variance (ANOVA) was used to examine the statistical differences across the four groups in changes in body weight over time and in escape latency to the platform during the water maze training trials, followed by Student–Newman–Keuls method to further detect between-group differences at each time point and at each trial. One-way ANOVA was used to detect statistical differences across the four groups in the behavioral variables of open-field testing and water maze probe testing. If the main effects reached significance, Student–Newman–Keuls method was further used for post hoc comparisons to detect between-group differences. Student's *t* test was used to examine statistical differences between the control and 10/10/40-mg/kg DAC groups in neuroimaging and cytokine variables. Data were expressed mean ± standard error of the mean (SEM). Intercorrelations among behavioral, in vivo neuroimaging, and cytokine variables were analyzed using linear regression; regression coefficients were obtained. SigmaPlot 13.0 software was used for statistical analysis. Statistical significance was defined as a P value of less than 0.05 with a two-sided test.

Results

Effects of DAC on Body Weight, Anxiety Level, and Locomotor Activity

There was a significant group × time interaction on the net change in body weight ($F_{3,60} = 2.940$, $P < 0.001$) with significant main effect of group ($F_{3,36} = 4.763$, $P = 0.007$) and time ($F_{20,720} = 9.937$, $P < 0.001$). Significant body weight loss was observed in mice treated with 10/10/40 and 15/15/60 mg/kg DAC on multiple treatment and recovery days compared with the control mice, but the body weight loss in the mice treated with 5/5/10 mg/kg DAC did not differ significantly from the control mice (Fig. 2S).

Open-field testing showed no significant differences across the four groups in the total distance traveled in the field ($F_{3,36} = 1.257$, $P = 0.306$), movement velocity ($F_{3,36} = 0.271$, $P = 0.846$), time spent in the central zone ($F_{3,36} = 0.175$, $P = 0.913$), and the frequency of entry into the central zone ($F_{3,36} = 0.311$, $P = 0.817$) (Fig. 3S).

Effects of DAC Regimens on Learning and Memory Abilities in Morris Water Maze Test

Five of the ten mice treated with the high dose of DAC (15/15/60 mg/kg) died during the water maze test. In the habituation trial, there was no any spatial bias and basal swim speed difference displayed (data not shown). In the training trials, treatment had a significant effect on the escape latency ($F_{3,167} = 3.599$, $P = 0.015$). The mice treated with 10/10/40 mg/kg DAC had a significantly longer escape latency on trial 4 than the control mice ($P = 0.043$) (Fig. 1a). In the probe test, significant main effects of group were observed for the duration spent in the targeted quadrant ($F_{3,31} = 7.170$, $P < 0.001$) and the frequency of entry into the targeted quadrant ($F_{3,31} = 0.105$, $P < 0.001$), but not for the movement of velocity ($F_{3,31} = 0.105$, $P = 0.956$). The mice treated with 5/5/20 and 10/10/40 mg/kg DAC had a significantly shorter duration spent in the targeted quadrant than the control mice ($P \leq 0.038$); the mice treated with 10/10/40 and 15/15/60 mg/kg DAC had significantly fewer entries into the targeted quadrant than the control mice

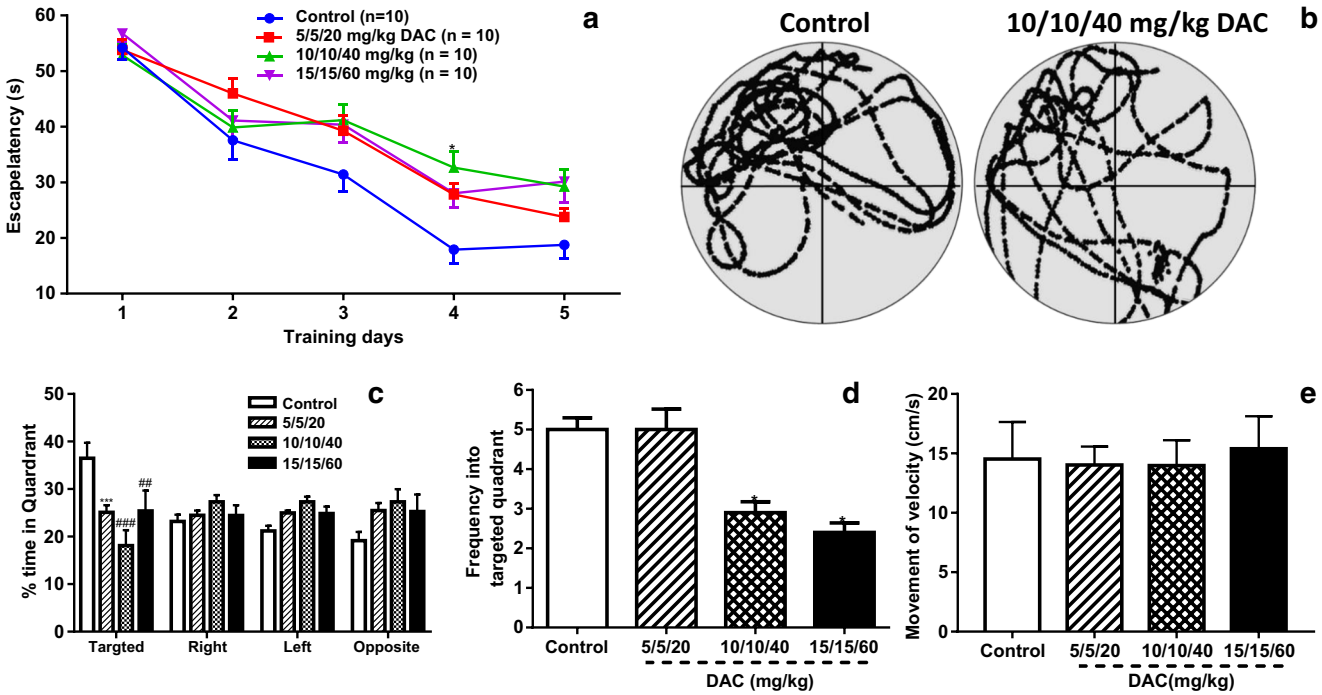

Fig. 1 The effects of DAC in water maze test. Escape latency to platform in training trials (**a**), duration stayed in four quadrants (**c**) and frequency (**d**) into the targeted quadrant, and mobility time in the maze (**e**) during probe test. Data are expressed as mean ± SEM and analyzed using one- or two-way ANOVA. $^{*}P < 0.05$, $^{**}P < 0.01$, $^{***}P < 0.001$ vs. controls. **b** shows representative tracking patterns of controlled and 10/10/40-mg/kg DAC-treated mice in probe test

($P \leq 0.002$) (Fig. 1). Due to the high mortality rate of 15/15/60 mg/kg and comparable cognitive impairment of mice treated with 10/10/40 mg/kg DAC, the dose of 10/10/40 mg/kg DAC was then chosen as the optimal dosing regimen for further in vivo neuroimaging and cytokine experiments.

Effects of DAC on Hippocampal MEMRI Intensity and Dendritic Spine Plasticity of Prefrontal Cortical Neurons

After the water maze test, the hippocampal neuronal activity of the mice treated with saline solution and those treated with 10/10/40 mg/kg DAC was further scanned by MEMRI. A significant decrease in the MEMRI signal intensity was observed in the dentate gyrus ($t_8 = 3.397$, $P = 0.009$), CA1 ($t_8 = 3.903$, $P = 0.005$), and CA3 ($t_8 = 3.040$, $P = 0.0161$) of the DAC-treated mice with the control mice (Fig. 2).

In two-photon microscopic experiments using Thy1-YFP H-line transgenic mice, those treated with 10/10/40 mg/kg DAC had a striking increase in dendritic spine elimination rate ($t_8 = 11.309$, $P = 0.000$) and a significant net loss of spines ($t_8 = 11.444$, $P = 0.000$) in the frontal association cortical neurons ($t_8 = 8.686$, $P = 0.000$) compared with the control group. DAC did not lead to effects on filopodia elimination, formation, and net change that led to differences from the control group (Fig. 3).

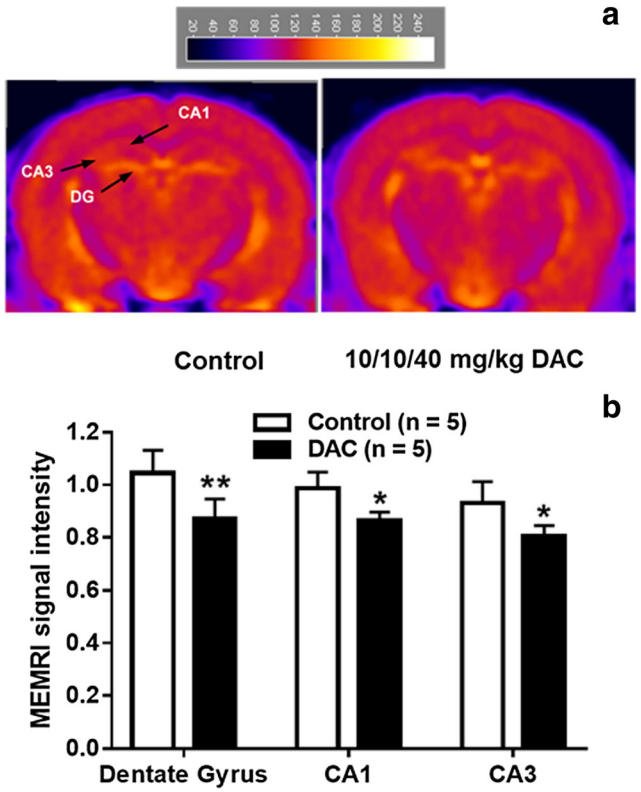

Fig. 2 The effects of 10/10/40 mg/kg DAC on MEMRI signal intensity in hippocampal subregions (**a**). Data are expressed as mean ± SEM and analyzed using Student's *t* test: $^{*}P < 0.05$, $^{**}P < 0.01$ vs. controls (**b**). *DG* dentate gyrus

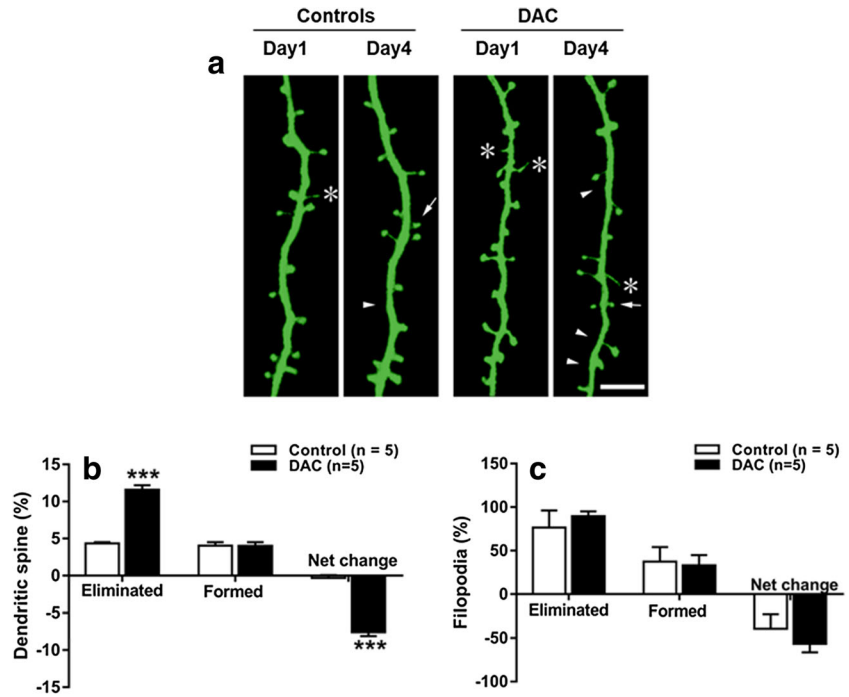

Fig. 3 The effects of 10/10/40 mg/kg DAC on two-photon microscopy-detected dendritic spines of the prefrontal cortical neurons in Thy1-YFP H-line transgenic mice (**a**). Percentages of eliminated, newly formed, and net change in spines (**b**) and filopodia (**c**). Data are expressed as mean ± SEM and analyzed using Student's *t* test: ***$P <$ 0.001 vs. controls. Newly formed, eliminated spines, and filopodia are indicated with arrows, arrowheads, and stars, respectively, in **a** (scale bar = 5 μm)

Effects of DAC on Serum and Brain Cytokine Levels

In C57/BL6J mice, the DAC-treated group had markedly higher concentrations of IL-6 in the whole brain ($t_{10} = 6.594$, $P <$ 0.0001) and in the hippocampus ($t_{10} = 9.512$, $P < 0.001$) and of TNF-α in all four tissues tested than those found in the control mice ($t_{10} \geq 5.306$, $P \leq 0.0003$). Both IL-4 and IL-10 were significantly decreased in the DAC-treated groups compared with the control mice ($t_{10} \geq 3.233$, $P \leq 0.009$) (Fig. 4). In transgenic mice, IL-6 and TNF-α were measured in serum, the prefrontal cortex, and the hippocampus. The DAC-treated group showed significantly higher concentrations of IL-6 in the hippocampus ($t_8 =$ 13.307, $P < 0.001$) and of TNF-α in all three tissues tested than those found in the control mice ($t_8 \geq 10.370$, $P \leq 0.001$) (Fig. 5).

Intercorrelations Between Behavioral, Neuroimaging, and Cytokine Variables

For the behavioral variables, the frequency into the targeted quadrant of the water maze showed significant positive correlation with the MEMRI signal intensity in CA1 ($r = 0.733$, $P =$ 0.016) and CA3 ($r = 0.645$, $P = 0.044$) (Table 1). A striking negative correlation was observed between the duration traveled in the targeted quadrant and the hippocampal IL-6 level ($r = -$ 0.871, $P < 0.001$). The IL-6 concentration of the whole brain also showed significant negative correlation with the duration ($r = -0.691$, $P = 0.013$) and frequency ($r = -0654$, $P = 0.021$). The serum TNF-α concentration showed significant inverse correlations with duration ($r = -0.829$, $P < 0.001$) and frequency ($r = -0.736$, $P = 0.006$). The TNF-α concentration of the prefrontal cortex and hippocampus also showed negative correlation with the duration ($r = -0.745$, $P = 0.005$; $r = -0.728$, $P =$ 0.007) and frequency ($r = -0.632$, $P = 0.028$; $r = -0.651$, $P =$ 0.022). While, positive correlation was observed between the duration in the targeted quadrant and IL-4 level in serum ($r =$ 0.733, $P = 0.007$), whole brain ($r = 0.591$, $P = 0.043$), and hippocampus ($r = 0.589$, $P = 0.044$). The frequency into the targeted quadrant showed positive correlation with serum IL-4 level ($r = 0.612$, $P = 0.034$). The serum IL-10 concentration demonstrated positive correlations with duration ($r = 0.607$, $P = 0.036$) and frequency ($r = 0.611$, $P = 0.035$). Besides, the duration in targeted quadrant also positive correlation with IL-10 level in hippocampus ($r = 0.689$, $P = 0.013$) (Table 1).

For the MEMRI variables, the whole-brain IL-6 and TNF-α concentrations showed significant inverse correlations with the MEMRI signal intensity in the dentate gyrus ($r \leq -$ 0.768, $P \leq 0.026$) and CA3 ($r \leq -0.751$, $P \leq 0.032$) (Table 2).

For the two-photon imaging studies, the percentage of spine elimination and the net loss of spines showed strong positive correlation with the hippocampal IL-6 concentration ($r \geq 0.927$, $P \leq 0.001$) and the serum, prefrontal, and hippocampal TNF-α levels ($r \geq 0.949$, $P < 0.001$). The blood IL-6 concentration also showed a significant correlation with the loss of spines ($r = 0.690$, $P = 0.027$) (Table 2).

Discussion

This study represents an investigation into chemotherapy-induced cognitive impairment and its associations with cytokine

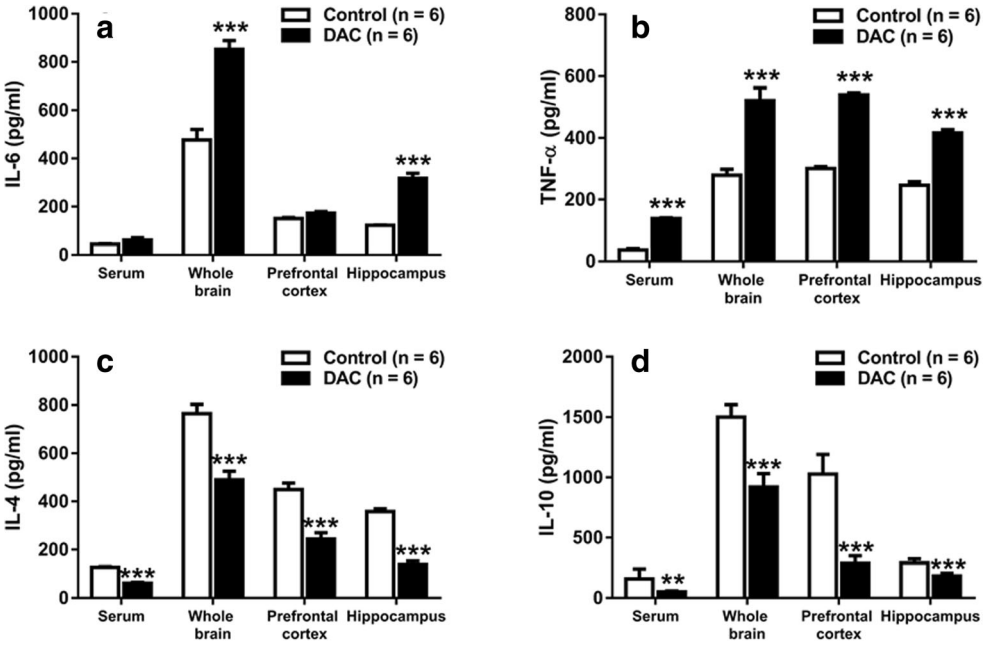

Fig. 4 The effects of 10/10/40 mg/kg DAC on cytokine levels of IL-6 (**a**), TNF-α (**b**), IL-4 (**c**), and IL-10 (**d**) in sera, whole brain, prefrontal cortex, and hippocampus of C57/BL6J mice. Data are expressed as mean ± SEM and analyzed using Student's *t* test: $^{*}P < 0.05$, $^{**}P < 0.01$, $^{***}P < 0.001$ vs. controls (**b**)

dysregulation and disruption in neuroplasticity with the use of behavioral, biochemical, and in vivo neuroimaging approaches.

Unlike most previous studies, in which single or common adjuvant chemotherapeutic agents were used to establish animal models of chemobrain [4, 5, 7], the combination regimen used in this study could produce more obvious behavioral deficits in a shorter treatment duration. Indeed, this study showed that the medium dose of DAC produced the most apparent cognitive impairment detected in the water maze test, which manifested as a longer escape latency to the platform during the training trials and as a shorter duration in and fewer entries into the targeted quadrant during the probe test. On the other hand, this study also observed significant body weight loss in the mice treated with the two higher doses of DAC; the highest dose even caused a remarkably high mortality rate in the transgenic mice. These toxic effects are consistent with cachexia and other related side effects often experienced by cancer patients undergoing chemotherapy [25]. Despite of this, no tested dose of DAC affected either locomotion or anxiety level, as evidenced by the lack of difference across the four groups in the total distance traveled and in the movement velocity in the open field and in the mobility time in the water maze; all of the groups spent similar amounts of time in the central zone and made similar numbers of entries into the central zone of the open field. These results indicate that body weight loss had limited influences on locomotor ability and anxiety level and cognitive deterioration observed in this study was a consequence of the toxic side effects of chemotherapy.

Previous studies have well demonstrated multiple mechanisms involved in hippocampal toxicity-related cognitive impairment [26]. The MEMRI data in this study revealed a broad decrease in neuronal activity across hippocampal subregions in DAC-treated mice. Moreover, the decreased MEMRI signal intensity in CA1 and CA3 was strongly correlated with fewer entries into the targeted quadrant in the water maze, which confirms an association of DAC-induced memory decline with decreased hippocampal neuronal activity. These results are also consistent with previous neuroimaging studies that suggest the potential role of the hippocampus in the pathogenesis of chemobrain [15, 27]. This study further showed striking dendritic spine elimination and a net loss in the medical

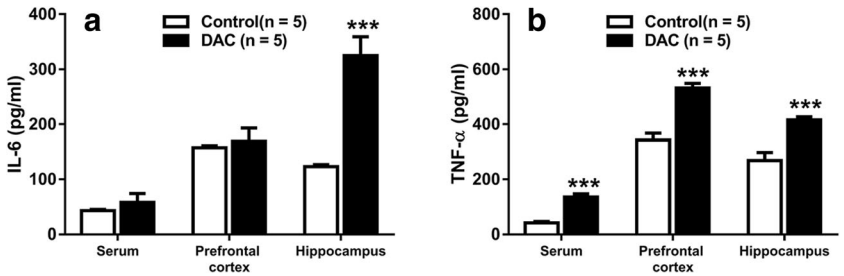

Fig. 5 The effects of 10/10/40 mg/kg DAC on cytokine levels of IL-6 (**a**) and TNF-α (**b**) in sera, prefrontal cortex, and hippocampus of Thy1-YFP transgenic mice. Data are expressed as mean ± SEM and analyzed using Student's *t* test: $^{***}P < 0.001$ vs. controls (**b**)

Table 1 Cognitive behavioral correlates with MEMRI signal intensity of hippocampal subregions and cytokines

	Duration		Frequency	
	r	*p*	*r*	*p*
Hippocampal MEMRI signal intensity				
Dentate gyrus	0.488	0.153	0.627	0.053
CA1	0.523	0.121	0.733	0.016
CA3	0.497	0.144	0.645	0.044
Cytokines				
IL-6, serum	− 0.188	0.558	− 0.216	0.501
IL-6, whole brain	− 0.691	0.013	− 0.654	0.021
IL-6, prefrontal cortex	− 0.539	0.071	− 0.418	0.175
IL-6, hippocampus	− 0.871	< 0.001	− 0.621	0.031
TNF-α, serum	− 0.829	< 0.001	− 0.736	0.006
TNF-α, whole brain	− 0.414	0.181	− 0.448	0.138
TNF-α, prefrontal cortex	− 0.745	0.005	− 0.632	0.028
TNF-α, hippocampus	− 0.728	0.007	− 0.651	0.022
IL-4, serum	0.733	0.007	0.612	0.034
IL-4, whole brain	0.591	0.043	0.475	0.118
IL-4, prefrontal cortex	0.551	0.063	0.446	0.146
IL-4, hippocampus	0.589	0.044	0.435	0.163
IL-10, serum	0.607	0.036	0.611	0.035
IL-10, whole brain	0.239	0.454	0.191	0.552
IL-10, prefrontal cortex	0.567	0.054	0.347	0.269
IL-10, hippocampus	0.689	0.013	0.489	0.107

Control mice ($n = 6$) and mice treated with 10/10/40 mg/kg DAC ($n = 6$) were pooled for correlation analysis. Regression coefficient (r value) and P value were obtained from linear regression. Statistically significant correlations are highlighted in red

MEMRI manganese-enhanced magnetic resonance imaging

prefrontal cortical neurons of DAC-treated mice. Similar histologic changes in dendritic spines have also been observed in the hippocampal neurons of rats after long-term treatment with cyclophosphamide [28] and cycloheximide, a protein synthesis inhibitor [29], which suggests that the hippocampus and prefrontal cortex are susceptible to long-term chemotherapy and neurotoxins. In addition to hippocampal synaptic plasticity that plays a crucial role in spatial memory formation [30], a large body of evidence confirms that interactions between the hippocampus and the medial prefrontal cortex are essential to encoding and retrieval of spatial memory [31–33]. Inactivation and lesions of the medial prefrontal cortex impaired spatial working memory and retrieval [34–37]. It therefore seems that chemotherapy-induced cognitive impairment is associated not only with hippocampal dysfunction but also with disrupted plasticity in the medial prefrontal cortex.

Although the relationship between alterations in the circulating levels of multiple cytokines and cognitive dysfunction in cancer patients has been extensively investigated [9], little is known about cytokine changes in the brain and their associations with chemotherapy-induced cognitive impairment and disruption in neural plasticity. This study found that DAC consistently and broadly increased proinflammatory cytokine (IL-6 and TNF-α) levels and lowered anti-inflammatory cytokine (IL-4 and IL-10) levels in not only the blood stream but also the whole brain, hippocampus, and prefrontal cortical brain regions in the two mouse strains. A similar increase in blood, hippocampal, and cerebral cortical TNF-α levels has been detected in rats treated with adriamycin [38], which confirms the chemotherapy-induced overproduction of proinflammatory cytokines and suppression of antiinflammatory cytokines in the central nervous system.

Furthermore, this study showed multiple strong correlations between the elevated IL-6 and TNF-α levels of the whole brain, hippocampus, and prefrontal cortex and the decreased cognitive variables in the water maze test, the reduced MEMRI-detected hippocampal neuronal activity, the increased dendritic spine

Table 2 Cytokine correlates with MEMRI signal intensity of hippocampal subregions and dendritic spine plasticity of prefrontal cortical neurons

Cytokines	MEMRI DG		MEMRI CA1		MEMRI CA3		Spine elimination		Spine loss	
	r	*p*	*r*	*p*	*r*	*p*	*r*	*p*	*r*	*p*
IL-6, serum	− 0.084	0.843	− 0.123	0.771	− 0.095	0.823	0.626	0.053	0.690	0.027
IL-6, whole brain	− 0.768	0.026	− 0.689	0.059	− 0.752	0.031				
IL-6, PFC							0.302	0.396	0.244	0.496
IL-6, HIP							0.967	< 0.001	0.927	0.001
TNF-α, serum							0.973	< 0.001	0.974	< 0.001
TNF-α, whole brain	− 0.821	0.012	− 0.613	0.106	− 0.751	0.032				
TNF-α, PFC							0.972	< 0.001	0.949	< 0.001
TNF-α, HIP							0.956	< 0.001	0.962	< 0.001

Control mice ($n = 5$) and mice treated with 10/10/40 mg/kg DAC ($n = 5$) were pooled for correlation analysis. Regression coefficient (r value) and P value were obtained from linear regression. Statistically significant correlations are highlighted in red

MEMRI manganese-enhanced magnetic resonance imaging, *PFC* prefrontal cortex, *HIP* hippocampus

elimination, and the net loss of the association cortical neurons. These results demonstrate close associations of chemotherapy-induced overproduction of IL-6 and TNF-α with cognitive impairment, neuronal dysfunction, and disrupted neural plasticity in the related brain regions. Studies have implied a potential role of central and peripheral IL-6 in cognitive dysfunction [39]. An elevated TNF-α concentration has been found to be associated with neuronal cell loss, alterations of cortical dendritic spine density, and cognitive impairment caused by minimal traumatic brain injury [40], heart failure [41], and systemic viral infection [42] in mice. Chemotherapy-induced cytokine dysregulation, particularly overproduction of proinflammatory cytokines in the brain, appears to be an important factor contributing to the development of chemobrain by disrupting neuroplasticity in the related brain regions.

Several limitations of this study should be noted. First, it did not examine hippocampal neuronal dendritic spines due to methodological limitations [23, 24] and failed to obtain behavioral data from the transgenic mice due to the high mortality rate. This hindered us to directly elucidate the relationship between changes in hippocampal plasticity and the severity of cognitive impairment from the transgenic mice. Second, this study examined the combination chemotherapeutic regimen, rather than single chemotherapeutic agents. Individual agents that might exert a major effect in inducing chemobrain could not be identified. Third, although multiple interrelationships between behavioral, neuroimaging, peripheral, and brain cytokine variables were observed, the causality is undetermined. Further investigations should focus on identifying brain regional distribution of chemotherapeutic drugs and their effects at subcellular and molecular levels of the brain neurons. Finally, like most previous studies [4–7], this study was also conducted in "healthy" animals, rather than tumor-bearing animals. One recent study has found that cognitive deficits were more severe in tumorigenic mice than healthy control mice following treatment with a combination chemotherapy regimen [8], suggesting that tumor growth may exacerbate the development of chemobrain. Whether there exists a synergistic interaction between tumor cells and chemobrain-related pathological factors deserves further investigations.

Collectively, this study demonstrates chemotherapy-induced cognitive impairment and its associations with cytokine dysregulation, decreased neuronal activity, and disrupted neuroplasticity. Our results provide useful information toward a better understanding of the pathophysiology of chemobrain.

Funding This study was supported by General Research Fund (GRF) of Research Grant Council of HKSAR (17115017 for Z.J.Z.).

Compliance with Ethical Standards

Conflict of Interest The authors declare that they have no conflict of interest.

References

1. Asher A (2011) Cognitive dysfunction among cancer survivors. Am J Phys Med Rehabil 90:S16–S26
2. Nelson CJ, Nandy N, Roth AJ (2007) Chemotherapy and cognitive deficits: mechanisms, findings, and potential interventions. Palliat Support Care 5:273–280
3. Matsuda T, Takayama T, Tashiro M, Nakamura Y, Ohashi Y, Shimozuma K (2005) Mild cognitive impairment after adjuvant chemotherapy in breast cancer patients–evaluation of appropriate research design and methodology to measure symptoms. Breast Cancer (Tokyo, Japan) 12:279–287
4. Seigers R, Fardell JE (2011) Neurobiological basis of chemotherapy-induced cognitive impairment: A review of rodent research. Neurosci Biobehav Rev 35:729–741
5. Seigers R, Schagen SB, Van Tellingen O, Dietrich J (2013) Chemotherapy-related cognitive dysfunction: Current animal studies and future directions. Brain Imaging Behav 7:453–459
6. Konat GW, Kraszpulski M, James I, Zhang HT, Abraham J (2008) Cognitive dysfunction induced by chronic administration of common cancer chemotherapeutics in rats. Metab Brain Dis 23:325–333
7. Winocur G, Henkelman M, Wojtowicz JM, Zhang H, Binns MA, Tannock IF (2012) The effects of chemotherapy on cognitive function in a mouse model: a prospective study. Clin Cancer Res 18: 3112–3121
8. Winocur G, Berman H, Nguyen M, Binns MA, Henkelman M, van Eede M, Piquette-Miller M, Sekeres MJ et al (2018) Neurobiological mechanisms of chemotherapy-induced cognitive impairment in a transgenic model of breast cancer. Neuroscience 369:51–65
9. Wang XM, Walitt B, Saligan L, Tiwari AF, Cheung CW, Zhang ZJ (2015) Chemobrain: a critical review and causal hypothesis of link between cytokines and epigenetic reprogramming associated with chemotherapy. Cytokine 72:86–96
10. Dantzer R, Meagher MW, Cleeland CS (2012) Translational approaches to treatment-induced symptoms in cancer patients. Nat Rev Clin Oncol 9:414–426
11. Chae JW, Ng T, Yeo HL, Shwe M, Gan YX, Ho HK, Chan A (2016) Impact of TNF-alpha (rs1800629) and il-6 (rs1800795) polymorphisms on cognitive impairment in Asian breast cancer patients. PLoS One 11:e0164204
12. Cheung YT, Ng T, Shwe M, Ho HK, Foo KM, Cham MT, Lee JA, Fan G et al (2015) Association of proinflammatory cytokines and chemotherapy-associated cognitive impairment in breast cancer patients: a multi-centered, prospective, cohort study. Ann Oncol 26: 1446–1451
13. Ganz PA, Bower JE, Kwan L, Castellon SA, Silverman DH, Geist C, Breen EC, Irwin MR et al (2013) Does tumor necrosis factor-alpha (TNF-alpha) play a role in post-chemotherapy cerebral dysfunction? Brain Behav Immun 30(Suppl):S99–S108
14. Braida D, Sacerdote P, Panerai AE, Bianchi M, Aloisi AM, Iosue S, Sala M (2004) Cognitive function in young and adult IL (interleukin)-6 deficient mice. Behav Brain Res 153:423–429
15. Simo M, Rifa-Ros X, Rodriguez-Fornells A, Bruna J (2013) Chemobrain: a systematic review of structural and functional neuroimaging studies. Neurosci Biobehav Rev 37:1311–1321
16. Kaiser J, Bledowski C, Dietrich J (2014) Neural correlates of chemotherapy-related cognitive impairment. Cortex 54:33–50
17. Au HJ, Golmohammadi K, Younis T, Verma S, Chia S, Fassbender K, Jacobs P (2009) Cost-effectiveness analysis of adjuvant docetaxel, doxorubicin, and cyclophosphamide (tac) for node-positive breast cancer: Modeling the downstream effects. Breast Cancer Res Treat 114:579–587
18. Smith RE, Anderson SJ, Brown A, Scholnik AP, Desai AM, Kardinal CG, Lembersky BC, Mamounas EP (2002) Phase ii trial

of doxorubicin/docetaxel/cyclophosphamide for locally advanced and metastatic breast cancer: results from NSABP trial bp-58. Clin Breast Cancer 3:333–340
19. Inoue T, Majid T, Pautler RG (2011) Manganese enhanced mri (memri): neurophysiological applications. Rev Neurosci 22:675–694
20. Yang J, Khong PL, Wang Y, Chu AC, Ho SL, Cheung PT, Wu EX (2008) Manganese-enhanced mri detection of neurodegeneration in neonatal hypoxic-ischemic cerebral injury. Magn Reson Med 59: 1329–1339
21. Josvay K, Winter Z, Katona RL, Pecze L, Marton A, Buhala A, Szakonyi G, Olah Z et al (2014) Besides neuro-imaging, the thy1-yfp mouse could serve for visualizing experimental tumours, inflammation and wound-healing. Sci Rep 4:6776
22. Mancuso JJ, Chen Y, Li X, Xue Z, Wong ST (2013) Methods of dendritic spine detection: from golgi to high-resolution optical imaging. Neuroscience 251:129–140
23. Sau Wan Lai C (2014) Intravital imaging of dendritic spine plasticity. Intravital 3:e944439
24. Lai CS, Franke TF, Gan WB (2012) Opposite effects of fear conditioning and extinction on dendritic spine remodelling. Nature 483: 87–91
25. Caillet P, Liuu E, Raynaud Simon A, Bonnefoy M, Guerin O, Berrut G, Lesourd B, Jeandel C et al (2016) Association between cachexia, chemotherapy and outcomes in older cancer patients: a systematic review. Clin Nutr (Edinburgh, Scotland)
26. Dietrich J, Prust M, Kaiser J (2015) Chemotherapy, cognitive impairment and hippocampal toxicity. Neuroscience 309:224–232
27. Kesler SR, Bennett FC, Mahaffey ML, Spiegel D (2009) Regional brain activation during verbal declarative memory in metastatic breast cancer. Clin Cancer Res 15:6665–6673
28. Acharya MM, Martirosian V, Chmielewski NN, Hanna N, Tran KK, Liao AC, Christie LA, Parihar VK et al (2015) Stem cell transplantation reverses chemotherapy-induced cognitive dysfunction. Cancer Res 75:676–686
29. Malheiros JM, Polli RS, Paiva FF, Longo BM, Mello LE, Silva AC, Tannus A, Covolan L (2012) Manganese-enhanced magnetic resonance imaging detects mossy fiber sprouting in the pilocarpine model of epilepsy. Epilepsia 53:1225–1232
30. Bannerman DM, Sprengel R, Sanderson DJ, McHugh SB, Rawlins JN, Monyer H, Seeburg PH (2014) Hippocampal synaptic plasticity, spatial memory and anxiety. Nat Rev Neurosci 15:181–192
31. Spellman T, Rigotti M, Ahmari SE, Fusi S, Gogos JA, Gordon JA (2015) Hippocampal-prefrontal input supports spatial encoding in working memory. Nature 522:309–314
32. Sapiurka M, Squire LR, Clark RE (2016) Distinct roles of hippocampus and medial prefrontal cortex in spatial and nonspatial memory. Hippocampus 26:1515–1524
33. Churchwell JC, Morris AM, Musso ND, Kesner RP (2010) Prefrontal and hippocampal contributions to encoding and retrieval of spatial memory. Neurobiol Learn Mem 93:415–421
34. Horst NK, Laubach M (2009) The role of rat dorsomedial prefrontal cortex in spatial working memory. Neuroscience 164:444–456
35. Jo YS, Park EH, Kim IH, Park SK, Kim H, Kim HT, Choi JS (2007) The medial prefrontal cortex is involved in spatial memory retrieval under partial-cue conditions. J Neurosci 27:13567–13578
36. Taylor CL, Latimer MP, Winn P (2003) Impaired delayed spatial win-shift behaviour on the eight arm radial maze following excitotoxic lesions of the medial prefrontal cortex in the rat. Behav Brain Res 147:107–114
37. Urban KR, Layfield DM, Griffin AL (2014) Transient inactivation of the medial prefrontal cortex impairs performance on a working memory-dependent conditional discrimination task. Behav Neurosci 128:639–643
38. Tangpong J, Cole MP, Sultana R, Joshi G, Estus S, Vore M, St Clair W, Ratanachaiyavong S et al (2006) Adriamycin-induced, TNF-alpha-mediated central nervous system toxicity. Neurobiol Dis 23: 127–139
39. Trapero I, Cauli O (2014) Interleukin 6 and cognitive dysfunction. Metab Brain Dis 29:593–608
40. Baratz R, Tweedie D, Wang JY, Rubovitch V, Luo W, Hoffer BJ, Greig NH, Pick CG (2015) Transiently lowering tumor necrosis factor-alpha synthesis ameliorates neuronal cell loss and cognitive impairments induced by minimal traumatic brain injury in mice. J Neuroinflammation 12:45
41. Meissner A, Visanji NP, Momen MA, Feng R, Francis BM, Bolz SS, Hazrati LN (2015) Tumor necrosis factor-alpha underlies loss of cortical dendritic spine density in a mouse model of congestive heart failure. J Am Heart Assoc 4:e001920
42. Garre JM, Silva HM, Lafaille JJ, Yang G (2017) Cx3cr1+ monocytes modulate learning and learning-dependent dendritic spine remodeling via TNF-alpha. Nat Med 23:714–722